NASA Technical Memorandum 83449


# Resin Selection Criteria for "Tough" Composite Structures



C. C. Chamis and G. T. Smith
*Lewis Research Center*
*Cleveland, Ohio*

Prepared for the
Twenty-fourth Structures, Structural Dynamics and Materials Conference
sponsored by the AIAA, ASME, ASCE, and AHS
Lake Tahoe, Nevada, May 2–4, 1983

NASA

TABLE OF CONTENTS

# RESIN SELECTION CRITERIA FOR "TOUGH" COMPOSITE STRUCTURES

by

C. C. Chamis and G. T. Smith

National Aeronautics and Space Administration
Lewis Research Center
Cleveland, Ohio 44135

## ABSTRACT

Resin selection criteria are derived using a structured methodology consisting of an upward integrated mechanistic theory and its inverse (top-down structured theory). These criteria are expressed in a "criteria selection space" which can be used to identify resin bulk properties for improved composite "toughness". The resin selection criteria correlate with a variety of experimental data including laminate strength, elevated temperature effects and impact resistance.

## INTRODUCTION

It is well known in the fiber composite community that resins (matrices) provide the composite with the capability to resist load by keeping the fibers in place. The capability of the resin to keep the fibers in place results from a combination of chemical, thermal, and mechanical interactions. These combined interactions produce the in-situ resin physical, hygral, thermal, and mechanical properties which provide the composite with the requisite structural integrity in service environments, in general, and in turbine engine service environments in particular. A structured methodology is needed which can be used, in a formal way, to identify bulk (neat) resin characteristics which translate to quantifiable composite structural/mechanical behavior. The result of such structured methodology will be a set of criteria (guidelines) which can be used in advance to screen and/or select resins with the desirable bulk properties in order to provide the specified composite properties. The objective of the proposed paper is to describe a new structured methodology developed at Lewis for assessing, evaluating and identifying desirable bulk resin characteristics for specified structural composite integrity (fatigue resistance, fracture toughness, impact resistance, compressive strength, buckling resistance, vibration frequencies, and "toughness").

The structured methodology is based on an upward integrated mechanistic theory consisting of composite micromechanics, composite macromechanics, laminate theory and structural/stress analyses and its inverse (a top-down structured theory). All these are used formally to identify the resin characteristics which have a significant effect on composite mechanical behavior. The structured methodology is developed by using mainly matrix notation. Expanded equations are summarized in figures with appropriate schematics to illustrate the simulation and define the notation. The notation is also summarized in the Appendix for convenience. The structured methodology is based on Lewis' research activities on this subject during the past decade (for example references 1 to 3). The references cited in the text mainly refer to Lewis' research. However, these references include relevant references from

the literature. The results obtained are summarized in convenient criteria as simple equation or ratio form which can be used to select resins a priori for improved and/or specific composite toughness.

## STRUCTURED METHODOLOGY

The structured methodology used to develop the resin selection criteria embodies composite micromechanics, composite macromechanics, combined stress failure criteria, laminate theory and structural/stress analysis. The structured methodology is integrated from composite mechanics upward to structural analysis in order to relate the structural response to constituent materials (fibers and matrix). It is then used in reverse, top-down, from structural to composite micromechanics. The structured methodology is described herein using a top-down approach in order to formally relate a specific structural response (for example displacement, stress intensity, stress wave propagation, impact resistance) to constituent material properties (fibers and resins). Resin and matrix are used interchangeably throughout this discussion.

### Structural Response

The mathematical model describing the general structural response of a structure is given, using matrix notation, by

$$[M]\{\ddot{u}\} + [C]\{\dot{u}\} + [K]\{u\} = \{F(t)\} \tag{1}$$

where $\{\ddot{u}\}$, $\{\dot{u}\}$ and $\{u\}$ are the acceleration, velocity, and displacement vectors, respectively; $[M]$, $[C]$, and $[K]$ are the mass, structural damping, and stiffness matrices, respectively; and $\{F(t)\}$ is the time dependent force vector. The natural frequencies and buckling resistance (buckling load) of a structure are described by special cases of equation (1), respectively,

$$\langle [K] - \omega^2[M] \rangle = [0] \tag{2}$$

$$\langle [K] - \lambda^2[I] \rangle = [0] \tag{3}$$

where $\omega$ is the structure's natural frequency associated with a specific vibration mode, $\lambda$ is the eigenvalue containing the buckling load of a specific buckled shape and $[I]$ is the identity or unit matrix. If it is further assumed that $[C]$ is proportional to $[K]$, ($[C] = \gamma[K]$), prior to any damage, then equation (1) can be written thus

$$[M]\{\ddot{u}\} + \gamma[K]\{\dot{u}\} + [K]\{u\} = \{F(t)\} \tag{4}$$

Equations (2) and (4) depend on composite material properties embodied primarily in $[M]$ and $[K]$ while equation (3) depends only on $[K]$. For

most structural epoxies the density is about the same.[4] Therefore, the major influence of the resin in the global structural response of a composite structure is through the stiffness matrix [K].

The global structural stiffness matrix [K] is an assemblage of local stiffnesses. The local stiffnesses are related to the force deformation relationships and the local geometry. The force deformation relationships for a composite laminate, including hygral (moisture) and thermal forces, are given by[2]

$$\begin{Bmatrix} \{N\} \\ \{M\} \end{Bmatrix} = \begin{bmatrix} [A] & [C] \\ [C]^T & [D] \end{bmatrix} \begin{Bmatrix} \{\epsilon_o\} \\ \{\mu\} \end{Bmatrix} - \begin{Bmatrix} \{N_T\} \\ \{M_T\} \end{Bmatrix} - \begin{Bmatrix} \{N_M\} \\ \{M_M\} \end{Bmatrix} \tag{5}$$

where $\{N\}$ and $\{M\}$ are the resultant force and moment vectors at the section, respectively. The subscripts T and M denote thermal and moisture forces. The reference plane strain vector is given by $\{\epsilon_o\}$ and the local curvatures by $\{\mu\}$. The arrays [A], [C], and [D] denote axial, coupled and bending stiffness, respectively. The various arrays on the right side of equation (5) for an $N_\ell$ ply laminate, using laminate theory[5], are given by

$$[A],\ [C],\ [D] = \sum_{i=1}^{N_\ell} \left\langle \left[ (Z_t - Z_b),\ \frac{1}{2}(Z_t^2 - Z_b^2),\ \frac{1}{3}(Z_t^3 - Z_b^3) \right] [R]^T [E]^{-1} [R] \right\rangle_i$$

$$\{N_T\},\ \{M_T\} = \sum_{i=1}^{N_\ell} \left\langle \left[ (Z_t - Z_b),\ \frac{1}{2}(Z_t^2 - Z_b^2) \right] \Delta T [R]^T [E] \{\alpha\} \right\rangle_i \tag{6}$$

$$\{N_M\},\ \{M_M\} = \sum_{i=1}^{N_\ell} \left\langle \left[ (Z_t - Z_b),\ \frac{1}{2}(Z_t^2 - Z_b^2) \right] \Delta m [R]^T [E] \{\beta\} \right\rangle_i$$

In equation (6), Z locates the $i^{th}$ ply through the thickness from a reference plane, [R] is the strain transformation matrix which defines the $i^{th}$ ply orientation (ply material axes) relative to the structural axes, [E] defines the ply stress-strain relationships, $\{\alpha\}$ the ply thermal expansion coefficients, and $\{\beta\}$ the ply moisture expansion coefficients. The relative changes $\Delta T$ and $\Delta m$ denote the changes in temperature and moisture, respectively, of the $i^{th}$ ply measured from a reference condition. The temperature and the moisture for the $i^{th}$ ply are determined by heat transfer and moisture diffusion analyses.

The important point to note from equation (5) is that the resin properties influencing structural response are reflected through the ply property arrays $[E]$, $\{\alpha\}$, and $\{\beta\}$. Another important point to note is that the top-down structured theory described by equations (1) to (6) predicts global structural response which is in very good agreement with experimental data. For example: 1) the natural frequencies and mode shapes predicted by equation (2) are in excellent agreement with experimental data for fiber composite fan blades[6] and hybrid composite blades[7]; 2) the buckling loads of anisotropic plates, including bending, stretching, and coupling, predicted by equation (3) are in good agreement with experimental data[8,9]; 3) the impact displacements predicted using equation (4) are in good agreement with the high-speed movie data for a large hybrid composite fan blade[7]; and 4) the hygrothermomechanical response of a variety of angleplied laminates predicted by equation (5) are in very good agreement with measured data[2]. This good agreement of the predicted various structural responses with experimental data verifies that the global structural response of composite structures is formally related to the ply properties $[E]$, $\{\alpha\}$, and $\{\beta\}$ in equation (6). These ply properties can be formally related to matrix properties by continuing the top-down structured theory through composite macromechanics, combined-stress failure criteria, and composite micromechanics as will be described later.

## Stress Intensity/Concentration

Experimental data from composite laminates with circular holes and slit type defects exhibit the same fracture characteristics. These characteristics are similar for tensile or compressive loads and for a variety of hygrothermal environments[10]. Typical results are shown in figure 1. Explicit equations are available which describe the stress concentration/intensity in the vicinity of a circular hole in an infinite composite angleplied laminate[11]. The equations, relevant to this top-down structured theory, are summarized in figure 2 with accompanying schematics.

It can be seen in figure 2 that the stress concentration ratio $(\sigma_{C\theta\theta}/\sigma_{Cxx})$ in the vicinity of the hole depends on the laminate properties $E_{C\theta\theta}$, $E_{Cxx}$, $E_{Cyy}$, $G_{Cxy}$, and $\nu_{Cxy}$. These properties are determined using the following laminate theory equation[5]

$$[E_C] = \frac{1}{t_C} \sum_{i=1}^{N_\ell} \langle t\,[R]^T[E][R] \rangle_i \qquad (7)$$

where $t_C$ is the laminate thickness and $t_i$ is the ply thickness. Comparing equations (7) and (6), it can be seen by inspection that $[E_C] = [A]/t_C$. Therefore, the stress concentrations in the laminate (composite-structure) are formally related to ply properties through equation (7) and the equations in figure 2. The hygrothermal effects on the stress concentration are determined from equation (5) since the local laminate stresses are related to $\{N\}$ and $\{M\}$, or $\{\varepsilon_0\}$ and $\{\mu\}$ as will be described later.

## Stress Wave Propagation

The speed (C) of the inplane stress wave propagation in an angleplied composite laminate in the X, Y, and XY (shear) directions, respectively, are given by

$$C_x = \left[\frac{gE_{cxx}}{\rho(1-\nu_{cxy}\nu_{cyx})}\right]\frac{1}{2} \tag{8}$$

$$C_y = \left[\frac{gE_{cyy}}{\rho(1-\nu_{cyx}\nu_{cxy})}\right]\frac{1}{2} \tag{9}$$

$$C_{xy} = \left[(gG_{cxy}/\rho)\right]\frac{1}{2} \tag{10}$$

where $g$ is the gravity acceleration, $\rho$ is the laminate density, $G$ is the shear modulus and the subscripts denote respective directions. The corresponding through-the-thickness normal and shear speeds, respectively, are given by

$$C_z = (gE_{czz}/\rho) \tag{11}$$

$$C_{xz} = (gG_{cxz}/\rho) \tag{12}$$

$$C_{yz} = (gG_{cyz}/\rho) \tag{13}$$

The speeds predicted by equations (8) to (13), except equation (11), have been correlated with experimental data[12]. These equations have also been used extensively to theoretically investigate stress wave propagation in angleplied laminates due to normal, oblique and edge impacts[13].

Theoretical predictions of stress wave propagation due to point impact require a contact law in general. One such law for an impacting elastic sphere is given by the following approximate relationships[14].

$$F = (4/3)(R_s)^{1/2}\left[\frac{E_s E_{czz}}{E_s + (1-\nu_s)E_{czz}}\right]\delta^{3/2} \tag{14}$$

where $F$ is the contact force, $R$ is the radius of the impacting sphere and $\delta$ is the local indentation. The subscript $s$ denotes impacting sphere properties.

Taken collectively, equations (8) to (14) show that stress wave propagation in composite laminates depends on the laminate properties E, G, $\nu$, and $\rho$. These laminate properties are formally related to ply properties through equation (6) as was already mentioned.

## Ply Strains and Stresses

In the top-down structured theory, the $i^{th}$ ply strains $\{\varepsilon_i\}$ are formally related to global variables $\{\varepsilon_0\}$ and $\{\mu\}$ by the following matrix equation.

$$\{\varepsilon_i\} = [R_i]\ \{\varepsilon_0\} - Z_i\ \{\mu\} \tag{15}$$

where the global variables are determined from structural analysis. The corresponding ply stresses are given by

$$\{\sigma_i\} = [E_i]\ \{\varepsilon\} - \Delta m\{\beta\} - \Delta T\{\alpha\}_i \tag{16}$$

For the special case of in-plane loads only, the ply stresses are formally related to laminate stresses $\{\sigma_C\}$ by

$$\{\sigma_i\} = [E_i][R_i][E_C]^{-1}\ \{\sigma_C\} \tag{17}$$

where $[E_C]$ is given by equation (7). Equation (17) is significant because it shows that the ply stresses depend on local ply properties $[E_i]$ as well as integrated laminate properties $[E_C]$. Equation (17) constitutes the ply stress influence coefficients for the case of in-plane loads only.

The ply strains and stresses determined from equations (15) and (16), or (17), are normally compared to ply fracture properties using available failure criteria such as ply:

maximum strain: $\{\varepsilon_i\} \leq \{\xi_\ell\}$ (18)

maximum stress: $\{\sigma_i\} \leq \{S_\ell\}$ (19)

or combined-failure stress criterion, for example[15]

$$F(\sigma_i, S_\ell, K_\ell) = 1 - \left[\left(\frac{\sigma_{\ell 11\alpha}}{S_{\ell 11\alpha}}\right)^2 + \left(\frac{\sigma_{\ell 22\beta}}{S_{\ell 22\beta}}\right)^2 + \left(\frac{\sigma_{\ell 12S}}{S_{\ell 12S}}\right)^2 - K_{\ell 12}\ \frac{\sigma_{\ell 11\alpha}\sigma_{\ell 22\beta}}{S_{\ell 11\alpha}S_{\ell 22\beta}}\right] \tag{20}$$

where $\sigma_i$ denotes the $i^{th}$ ply stress along the material axes denoted by the numerical subscripts and with sense denoted by $\alpha$ or $\beta$ (tension or

compression). The corresponding ply uniaxial strengths (fracture stresses) are denoted by S. The coupling coefficient $K_{\ell 12}$ depends on the ply elastic properties $E_{\ell 11}$, $E_{\ell 22}$, $\nu_{\ell 12}$, and $\nu_{\ell 23}$.

The ply elastic constants $[E_\ell]$ and the uniaxial strengths $(S_\ell)$ can be formally related to matrix material properties using composite micromechanics as will be described subsequently.

Equations (18), (19), and/or (20) are used to assess laminate/composite structural integrity, durability, and/or composite toughness. This may be stated as the magnitude of stress $\{\sigma_c\}$, resulting from stress concentration due to impact or defects, that a composite can sustain prior to ply or interply damage which will degrade (1) the composite global structural response or (2) the composite life/durability[3]. The composite life, or durability, is usually measured by its resistance to cyclic (fatigue), mechanical, hygral, and/or thermal loading.

## Composite Micromechanics

Composite micromechanics is the discipline which formally relates ply properties to constituent material properties[4]. The properties pertinent to the development of "resin selection criteria" pursued herein are the ply mechanical properties (elastic $[E_\ell]$ and strength $S_\ell$) and the ply hygrothermal properties ($\beta_\ell$ and $\alpha_\ell$) where the subscript $\ell$ (instead of i) has been used to denote ply properties, in general. In addition, the hygrothermal degradation effects on the mechanical and thermal properties are related to the "hot-wet" ply environment and to the "hot-wet" glass transition temperature of the resin through a hygrothermal degradation factor Fm (HGTM).

The equations for predicting ply properties in terms of constituents are summarized in figure 3. The notation in these equations corresponds to the schematic in the figure. The ply elastic properties are explicitly related to the matrix (resin) (r) and fiber (f) properties and to the hygrothermal degradation through (Fm). It can be readily observed in these equations that the "resin-controlled" ply properties are: $E_{\ell 22}$, $E_{\ell 33}$, $G_{\ell 12}$, and $G_{\ell 23}$. The equations for ply longitudinal strengths (tension and compression) with attendant schematics for various fracture modes are summarized in figure 4. The dependence of the ply longitudinal compression strength on resin is through the resin properties (denoted by subscript (r)) and the ply intralaminar shear strength ($S_{\ell 12S}$). The hygrothermal degradation effects on ply longitudinal strengths are incorporated through the respective resin properties using the degradation factor (Fm) as shown in figure 3. Similarly, the equations for ply transverse (tension and compression) and intralaminar shear properties are summarized in figure 5. The equation for lower bound strength is derived assuming a resin slab (plate) perforated with a regular array of holes. The correlation between this equation and experimental data on yield stress of a steel plate[16] is illustrated in figure 6, where $S_p$ and $S$ denote yield stresses of the plate with and without the perforations, respectively. The parameter $R_{pa}$ denotes perforated area ratio which equals $K_f$ or the fiber volume ratio. The corresponding equations for ply hygral $(\beta_\ell)$ and thermal $(\alpha_\ell)$ properties are summarized in figure 7.

The equations summarized in figures 4, 5, and 6 close the loop in the structured methodology required to develop the "resin selection criteria".

Recall that this methodology consists of two multilevel theories: (1) An upward integrated theory which formally integrates resin elastic, hygral and thermal properties into composite structural response and (2) a top-down structured theory which formally relates the composite structural integrity/durability to the same resin and, in addition, strength properties. The hygrothermal environment and degradation effects are included in both theories.

## RESIN SELECTION CRITERIA--DERIVATIONS AND IDENTIFICATIONS

The resin selection criteria are derived with the aid of equations (17) and (20). Equation (17) is used in the form of Ply Stress Influence Coefficients (PSIC) defined as

$$[\mathscr{S}_\ell] = [E_\ell][R_i][E_c]^{-1} \tag{21}$$

where the subscript $\ell$ is again used to denote ply properties in general. The expanded form of equation (2) when the composite is subjected only to $\sigma_{cxx}$ is shown in figure 8. Analogous equations can be derived when the composite is subjected to other stresses or combinations[17]. Using the PSIC from the equations (fig. 8), equation (20), accounting for hygrothermal degradation effects ($\mathscr{F}_m$) and hygrothermomechanical degradation effects ($\mathscr{F}_{HTM}$), and rearranging results in the equation summarized in figure 9. The definitions for $\mathscr{F}_m$ and $\mathscr{F}_{HTM}$ are included at the bottom of the figure for completeness. The equation in this figure explicitly relates ply combined stress failure/damage (first ply failure) to the composite stress and includes the hygrothermomechanical degradation effects. The resin influence is through the properties with subscripts 22 and 12 and can now be readily assessed by expressing these properties in terms of constituent properties using the appropriate composite micromechanics equations from figures 3, 4, and 5.

The results obtained for transverse strength, transverse modulus, energy density and first ply failure, respectively, are summarized in figure 10. All of these are expressed explicitly in terms of matrix properties. The benefits of a matrix (resin) ($S_m$, $E_m$) relative to a reference matrix ($S_{mo}$, $E_{mo}$) are indicated by $\lambda_S$ ($S_m/S_{mo}$) for strength and $\lambda_m$ ($E_m/E_{mo}$) for modulus. The meaning of the parameters $C_s$, $C_m$, $C_o$, and $C$ is apparent from the equations in which they appear. These parameters are used to include those constituent material and ply properties which are independent, or very nearly so, of resin properties. Analogous expressions can be obtained for shear and interply delamination from the expressions in figure 10 by suitable replacement of variables and subscripts.

From the previous discussion and the expressions in figure 10, the resin selection criteria for improvements in individual properties are:

1. $\lambda_S$ for ply transverse and intralaminar shear strengths, for interply delamination and interlaminar shear controlled longitudinal compression.

2. $\lambda_m$ for ply transverse modulus, longitudinal tensile and shear strengths, and crippling-controlled longitudinal compression strength.

3. $\lambda_s/\lambda_m$ for ply transverse, intralaminar and interlaminar shear energy densities.

4. $\lambda_s/\lambda_m$ for laminate (composite) strength and "composite toughness" in general.

The graphical representation of the "resin selection criteria" is illustrated in figure 11 where the improvements relative to a reference (state-of-the-art), $S_{mo}$ and $E_{mo}$) matrix for individual and combined properties are readily observed. The "resin selection criteria" for improved "composite toughness" and structural integrity/durability in general can be now simply stated as follows:

"To improve composite toughness, increase the $S_m/E_m$ ratio relative to $S_{mo}/E_{mo}$ with $S_m$ increasing at a faster rate than $E_m$".

It is important to note that $S_m/E_m$ may be misconstrued as only strain to fracture. It is not as is readily observed from figure 12. It is also worth noting that the structural integrity dependence on the $(S_m/E_m)$ ratio is consistent with those obtained by sensitivity analyses in conjunction with structural optimization[18].

## COMPARISON WITH EXPERIMENTAL DATA AND DISCUSSION

Available experimental data[19, 20] for several composite properties made from a variety of resins, with stress strain curves as plotted in figure 13 and in different environments, are compared with the "resin selection criteria" described previously.

Angleplied laminate and unidirectional strengths and moduli are compared with $\lambda_m$ and $\lambda_s$ in figure 14. The correlation for resin-controlled properties (transverse and shear) with $\lambda_s$ is excellent. Also the fiber controlled strengths $S_{\ell 11F}$ (longitudinal flexure), $S_{\ell 11C}$ and $S_{CXX}$ correlate with $\lambda_m$. As expected, the fiber-controlled property $S_{\ell 11T}$ does not correlate with $\lambda_m$. A very good correlation of resin controlled properties (90° (transverse) and shear) with $\lambda_m$ only is shown in figure 15. Comparisons with elevated temperature data are shown in figure 16. Again the correlation of resin controlled properties (transverse and shear) with $\lambda_s$ is excellent, while there is no correlation of fiber controlled properties with $\lambda_m$.

Various resins, including those from figure 13, are plotted in the resin selection criteria space shown in figure 17. It can be seen in this figure that 5208 matrix is below the first ply failure boundary and would, therefore, be unsuitable for improved fracture toughness. A group of resins, however, are identified which will improve significantly the "composite toughness". These resins have $\lambda_s$ ratios of about 3 and $\lambda_m$ of about 2 or $\lambda_s/\lambda_m$ of about 1.5. The delaminated area sustained by a composite under impact loading is correlated with the resin selection criteria $\lambda_s/\lambda_m$ in figure 18. As can be seen, the correlation is excellent.

The important conclusion from the correlation results and discussion is that the "resin selection criteria" derived herein correlates with experimental data for a variety of conditions. The resin selection criteria space is a

concise graphical means to a priori identify resins with desirable bulk state characteristics which will lead to "tougher" composites. The correlation of the criteria with fatigue data is yet to be determined. However, based on the theoretical results, it is anticipated that these resin selection criteria should apply to fatigue loadings as well.

## CONCLUSIONS

Resin selection criteria for tougher composites were derived using a formal methodology consisting of upward integrated and top-down structured theories. The criteria account for resin strength and modulus, ply energy density, laminate first ply failure, environmental and cyclic load effects. The criteria are expressed in resin properties benefits regions where the region boundaries are given by simplified equations, or ratios, for resin strength and modulus. The resin selection criteria correlates with experimental data for a variety of conditions including laminate strength and stiffness, elevated temperature effects and resistance to impact. The criteria, expressed in a "criteria selection space", provide a formalized direction for the a priori selection and the development of resins for "tougher" composites.

## REFERENCES

1. Chamis, C. C.; Hanson, M. P.; and Serafini, T. T., "Criteria for Selecting Resin Matrices for Improved Composite Strength," Modern Plastic , vol. 50, no. 5, May 1973, p. 90.
2. Chamis, C. C.; Lark, R. F.; and Sinclair, J. H., "Integrated Theory for Predicting the Hydrothermomechanical Response of Advanced Composite Structural Components," Advanced Composite Materials - Environmental Effects, edited by J. R. Vinson, ASTM STP-658, American Society for Testing and Materials, Philadelphia, 1978, pp. 160-192.
3. Chamis, C. C.; and Sinclair, J. H., "Durability/Life of Fiber Composites in Hygrothermomechanical Environments," NASA TM-82749, 1981.
4. Chamis, C. C., "Simplified Composite Micromechanics Equations for Hygral, Thermal and Mechanical Properties,: SPI 38th Annual Conference, Houston, Texas, Feb. 1983.
5. Chamis, C. C.; "Computerized Multilevel Analysis for Multilayered Fiber Composites," Computers and Structures, Vol. 3, No. 3, May 1973, pp. 467-482.
6. Chamis, C. C., "Vibration Characteristics of Composite Fan Blades and Comparison with Measured Data," Journal of Aircraft, Vol. 14, No. 7, July 1977, pp. 644-647.
7. Chamis, C. C.; and Sinclair, J. H., "Analysis of High Velocity Impact on Hybrid Composite Fan Blades," Journal of Aircraft, Vol. 17, No. 10, Oct 1980, pp. 763-766.
8. Chamis, C. C., "Buckling of Anisotropic Composite Plates, "Journal of the Structural Division, ASCE, Vol. 95, No. ST10, Oct. 1969, pp. 2119-2139.
9. Ashton, J. E.; and Whitney, J. M., Theory of Laminated Plates, Technomic Publishing Co., Westport, CT., 1970.
10. Porter, T. R., "Environmental Effects on Defect Growth in Composite Materials,: NASA CR-165213, 1981.
11. Lekhnitskii, S. G., Anizotropnye Plastinki (Anisotropic Plates), Translated from the 2nd Russian Ed., by S. W. Tsai and T. Cheron, Gordon and Breach, New York, 1968, p. 457.

12. Daniel, I. M.; and Liber, T., "Wave Propagation in Fiber Composite Laminates," IIT Research Inst., Chicago, ILL., IITRI-D6073-3-PT-2, June 1976. (NASA CR-135086).
13. Kim, B. S.; and Moon, F. C., "Impact on Multilayered Composite Plates," NASA CR-135274, 1977.
14. Yang, S. H.; and Sun, C. T., "Indentation Law for Composite Laminates," Purdue Univ., Lafayette, Ind., CML-81-1, July 1981. (NASA CR-165460).
15. Chamis, C. C., "Failure Criteria for Filamentary Composites," Composite Materials-Testing and Design, ASTM STP-460, American Society for Testing and Materials, Philadelphia, 1969, pp. 336-351.
16. Unpublished Lewis Research Center Results, 1981.
17. Chamis, C. C., "Prediction of Fiber Composite Mechanical Behavior Made Simple," Rising to the Challenge of the 80's, Society of the Plastics Industry, Inc., New York, 1980, pp. 12-A-1 to 12-A-10.
18. Chamis, C. C., "Sensitivity Analysis Results of the Effects of Various Parameters on Composite Design," SAMPE Quaterly, Vol. 14, No. 2, Jan 1983, pp. 1-6.
19. Browning, C. E.; Husman, G. E.; and Whitney, J. M., "Moisture Effects in Epoxy Matrix Composites," Composite Materials-Testing and Design, ASTM STP-617, American Society for Testing and Materials, Philadelphia, 1977, pp. 481-496.
20. Palmer, R. J., "Investigation of the Effect of Resin Materials on Impact Damage to Graphite/Epoxy Composites," NASA CR-165677, 1981.

## SYMBOLS

| | |
|---|---|
| A | laminate axial stiffness |
| C | global damping matrix; laminate stiffness matrix; stress wave speed |
| D | laminate bending stiffness |
| E | elastic properties matrix as defined by subscripts; modulus, as defined by subscripts |
| F | global force; failure criterion function |
| $\mathcal{F}$ | hygrothermal property degradation factor |
| g | gravity acceleration |
| I | Identity Matrix |
| i | index |
| $\mathcal{J}$ | ply stress influence coefficient as defined by subscripts |
| K | global stiffness matrix; coupling coefficient in failure criterion |
| M | global mass matrix; laminate moment as defined by subscripts |
| m | moisture |
| N | laminate in-plane force as defined by subscripts |
| $N_\ell$ | number of layers in a laminate |
| R | ply orientation matrix; impacting sphere radius |
| S | strength as defined by subscripts |
| T | temperature |
| t | thickness as defined by subscripts |
| u | global displacement |
| x,y,z | global (structural axes) coordinates |
| 1,2,3 | ply material axes coordinates |
| $\alpha$ | thermal expansion coefficient as defined by subscripts |
| $\beta$ | moisture expansion coefficient as defined by subscripts |
| $\gamma$ | global damping matrix proportionality factor |
| $\Delta$ | change |
| $\delta$ | local indentation |
| $\epsilon$ | strain as defined by subscripts |
| $\epsilon_0$ | global reference plane strain |
| $\xi$ | failure strain as defined by subscripts |
| $\lambda$ | eigenvalue; resin selection criteria ratio as defined by subscript |
| $\mu$ | global curvatures as defined by subscripts |
| $\nu$ | Poisson's ratio as defined by subscripts |
| $\rho$ | density as defined by subscripts |

| | |
|---|---|
| $\sigma$ | stress as defined by subscripts |
| $\varphi$ | nondimentional function defined by appropriate equations |
| $\omega$ | circular frequency |

Subscripts

| | |
|---|---|
| C | compression |
| c | composite property |
| HTM | hygrothermomechanical effect |
| $\ell$ | ply property |
| m | moisture, hygrothermal effects |
| r | resin property |
| S | shear |
| s | sphere |
| T | tension, temperature |
| xyz | respective coordinate directions, properties |
| 123 | ply material axes respective properties |
| $\alpha$ | T-tension or C-compression |
| $\beta$ | T-tension or C-compression |

Matrices

| | |
|---|---|
| $[\ ]$ | array, matrix |
| $\{\ \}$ | vector, column matrix |
| $[\ ]^{-1}$ | matrix inverse |
| $[\ ]^{T}$ | matrix transpose |

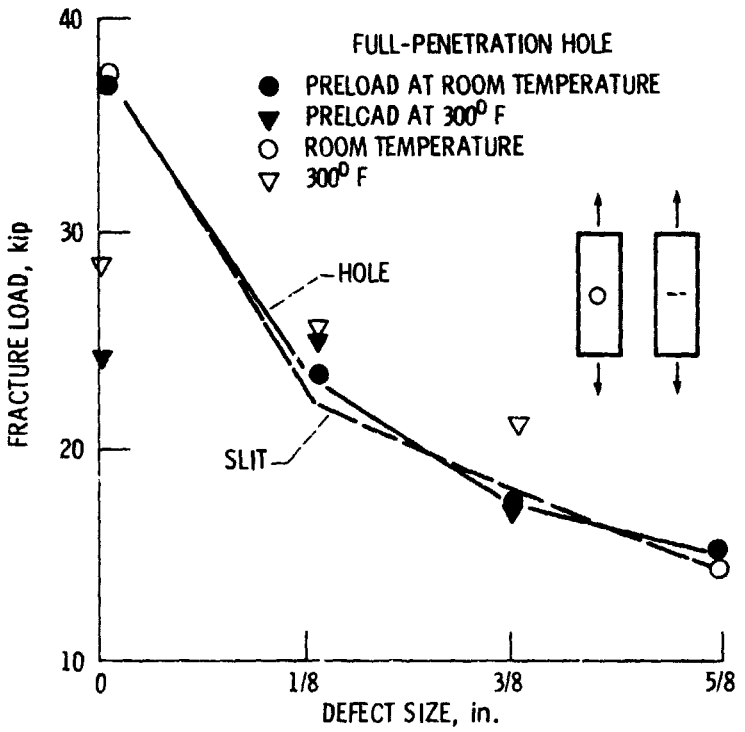


Figure 1. - Defected laminate static fracture data.

$$\frac{\sigma_{c\theta\theta}}{\sigma_{cxx}} = \frac{E_{c\theta\theta}}{E_{cxx}} \left\{ R_0 \left[ (R_0 + R_{DI}) \sin^2\varphi \right] \cos^2\theta + \left[ (1 + R_{DI}) \cos^2\varphi \right] \sin^2\theta - \frac{R_{DI}}{4} (1 + R_0 + R_{DI}) \sin 2\varphi \sin 2\theta \right\}$$

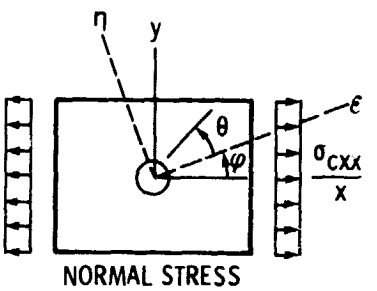

NORMAL STRESS

$$R_0 = \sqrt{E_{cxx}/E_{cyy}}$$

$$R_{DI} = \left[ 2\left( \frac{E_{cxx}}{E_{cyy}} - \upsilon_{cxy} \right) + \frac{E_{cxx}}{G_{cxy}} \right]^{1/2}$$

$$\frac{\sigma_{c\theta\theta}}{\sigma_{cxy}} = \frac{E_{c\theta\theta}}{2E_{cxx}} \left\{ (1 + R_0 + R_{DI}) - R_{DI} \cos 2\varphi \sin 2\theta + \left[ (1 + R_0) \cos 2\theta + R_0 - 1 \right] \sin 2\varphi \right\}$$

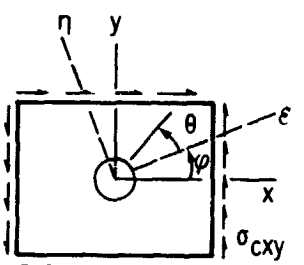

SHEAR STRESS

NOTE: $\sigma_{c\theta\theta}$ AND $E_{c\theta\theta}$ ARE IN THE HOOP DIRECTION AT $\theta$

Figure 2. - Stress concentrations depend significantly on composite moduli.

$$F_m = \left[ \frac{T_{gwr} - T_T}{T_{gro} - T_{ro}} \right]^{1/2}$$

$$E_{\ell 11} = k_f E_{f11} + k_r F_m E_{ro}$$

$$\upsilon_{\ell 12} = \upsilon_{\ell 13} = k_f \upsilon_{f12} + k_r \upsilon_{ro}$$

$$E_{\ell 33} = E_{\ell 22} = \frac{F_m E_{ro}}{1 - \sqrt{k_f}\left(\frac{1 - F_m E_{ro}}{E_{f22}}\right)}$$

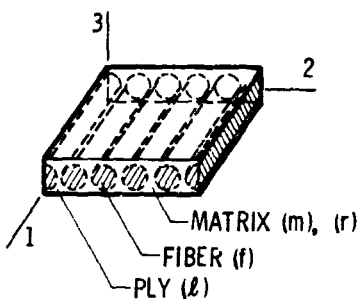


$$G_{\ell 13} = G_{\ell 12} = \frac{F_m G_{ro}}{1 - k_f (1 - F_m G_{ro}/G_{f23})}$$

$$G_{\ell 23} = G_{\ell 32} = \frac{F_m G_{ro}}{1 - k_f (1 - F_m G_{ro}/G_{f23})}$$

$$\upsilon_{\ell 23} = (E_{\ell 22}/2G_{\ell 23}) - 1$$

Figure 3. - Governing equations: micromechanics-elastic continued.

$$S_{\ell 11T} = S_{ft}\left[\beta_{ft} k_f + k_r E_r / E_{f11}\right]$$

$$S_{\ell 11C} = \text{MIN}\left\{ S_{fc}\left(\beta_{fc} k_f + k_r E_r / E_{f11}\right),\ S_{rc}\left(k_r + \beta_{fc} k_f E_{f11} / E_r\right),\right.$$

$$\left.\left[\frac{F(k_v)\, G_r}{(1 - k_f) + k_f G_r / G_{f12}}\right],\ \left(\beta_{cs} S_{\ell 12S} + S_{rc}\right)\right\}$$

$$F(k_v) = \frac{1 - 2\left(\frac{k_v}{1-k_f}\right) + \left(\frac{k_v}{1-k_f}\right)^2}{1 - \left(\frac{k_v}{1-k_v}\right)}$$

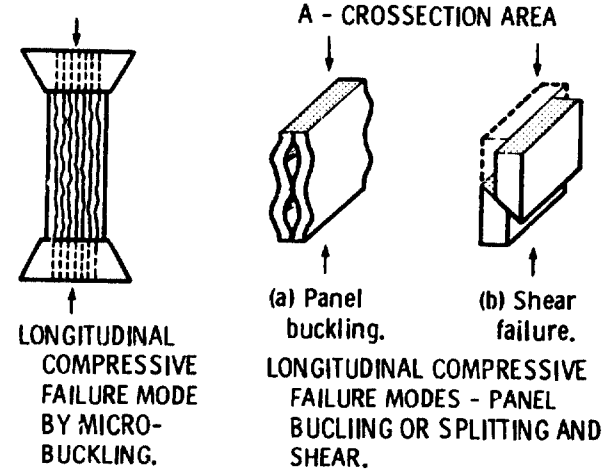


Figure 4. - Governing equations: micromechanics-uniaxial strengths.

TRANSVERSE

$$S_{\ell 22T,\,C} = \frac{1}{\left[1 - \sqrt{k_f}\left(\frac{1 - E_m}{E_{f22}}\right)\right]\left[1 + \varphi_\eta(\omega_\eta - 1) + 1/3(\varphi_\eta - 1)^2\right]^{1/2}} S_{MT,\,C}$$

$$\varphi_\eta = \frac{1}{\left(\frac{\pi}{4k_f}\right)^{1/2} - 1}\left[\left(\frac{\pi}{4k_f}\right)^{1/2} - \frac{1}{1 - \sqrt{k_f}\left(\frac{1 - E_m}{E_{f22}}\right)}\left(\frac{E_m}{E_{f22}}\right)\right]$$

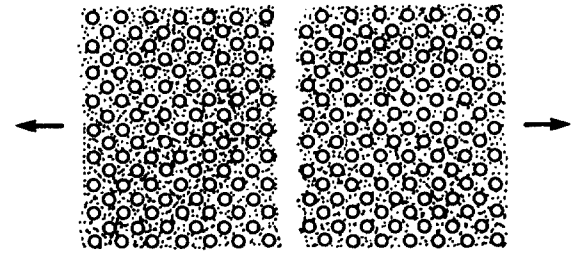

SCHEMATIC OF TRANSVERSE FAILURE

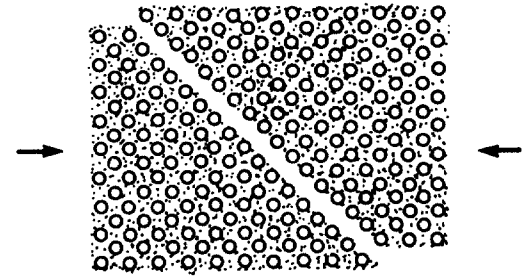

SCHEMATIC OF TRANSVERSE COMPRESSIVE FAILURE MODE

LOWER BOUND

$$S_{\ell 22T,\,C} = \left[1 - \left(\frac{4k_f}{\pi}\right)^{1/2}\right] S_{MT,\,C}$$

INTRALAMINAR SHEAR: REPLACE E & $S_{MT}$ WITH G & $S_{MS}$, RESPECTIVELY

VOID EFFECTS: $S_{MV} = \left\{1 - [4k_v/(1 - k_f)\pi]^{1/2}\right\} S_M$

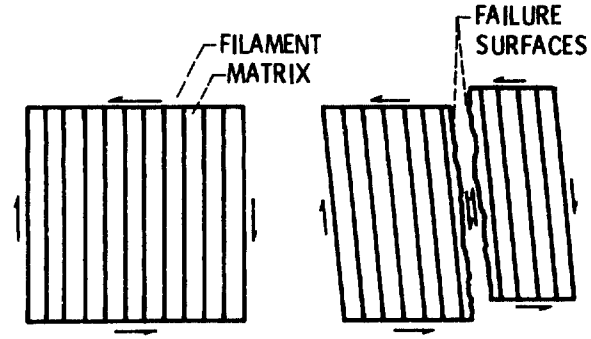


SCHEMATIC OF SHEAR FAILURE MODES (INPLANE, INTRALAMINAR)



Figure 5. - Governing equations: micromechanics-uniaxial strengths continued.

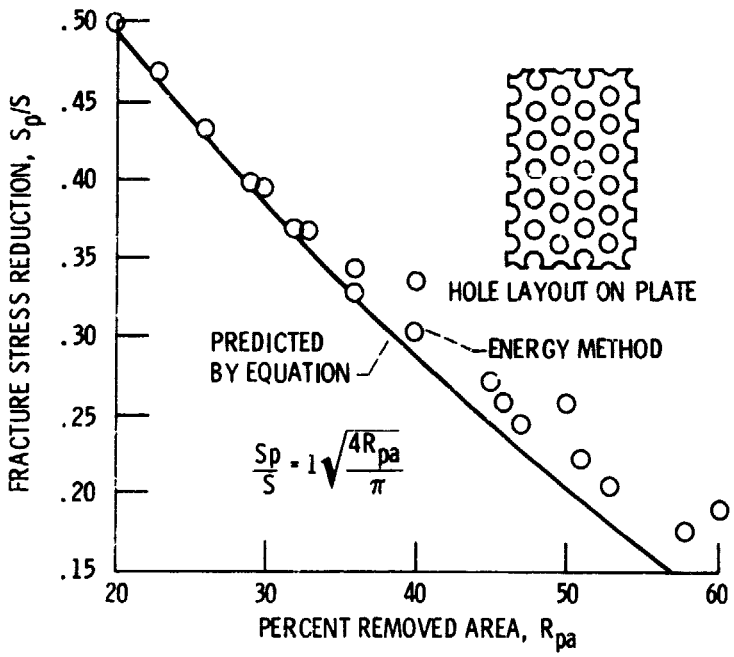


Figure 6. - Simple expression accurately predicts fracture stress reduction in perforated plates compared to energy method.

MOISTURE EXPANSION COEFFICIENTS

$$\beta_{\ell 11} = \beta_r \, (1 - k_f) \, E_r / E_{f11}$$

$$\beta_{\ell 22} = \beta_r \left(1 - \sqrt{k_f}\right)\left[1 + \frac{\sqrt{k_f}\left(1 - \sqrt{k_f}\right) E_r}{\sqrt{k_f}\, E_{\ell 22} + \left(1 - \sqrt{k_f}\right) E_r}\right] = \beta_{\ell 33}$$

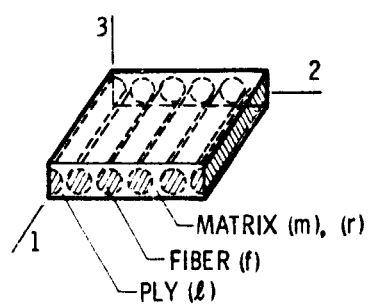


THERMAL EXPANSION COEFFICIENTS

$$\alpha_{\ell 11} = \left(k_f \alpha_{f11} E_{f11} + k_r \alpha_r E_r\right) / E_{\ell 11}$$

$$\alpha_{\ell 22} = \alpha_{f22} \sqrt{k_f} + \left(1 - \sqrt{k_f}\right)\left(1 + k_f \nu_r E_{f11} / E_{\ell 11}\right) \alpha_r = \alpha_{\ell 33}$$

Figure 7. - Governing equations: micromechanics-hygrothermal properties.

$$\mathcal{I}_{L/X} = \frac{E_{\ell 11}}{E_{cxx}\,(1 - \nu_{\ell 12}\,\nu_{\ell 21})}\left[(1 - \nu_{\ell 21}\,\nu_{cxy})\cos^2\theta + (\nu_{\ell 21} - \nu_{cxy})\sin^2\theta\right]$$

$$\mathcal{I}_{T/X} = \frac{E_{\ell 22}}{E_{cxx}\,(1 - \nu_{\ell 12}\,\nu_{\ell 21})}\left[(\nu_{\ell 12} - \nu_{cxy})\cos^2\theta + (1 - \nu_{cxy}\,\nu_{\ell 21})\sin^2\theta\right]$$

$$\mathcal{I}_{S/X} = \frac{G_{\ell 12}}{E_{cxx}\,(1 - \nu_{\ell 12}\,\nu_{\ell 21})}\left[(1 + \nu_{cxy})\sin^2\theta\right]$$

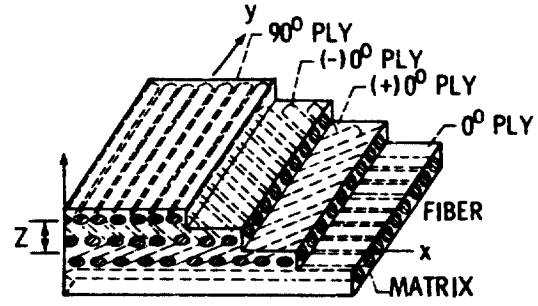


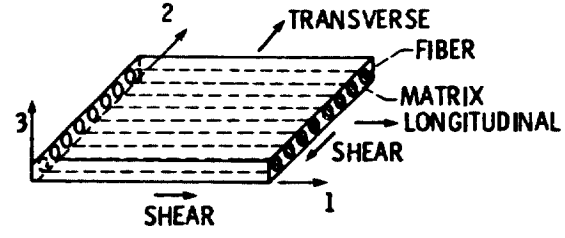


WHERE

$\sigma_{\ell 11} = \mathcal{I}_{L/X}\,\sigma_{cxx}$; $\sigma_{\ell 22} = \mathcal{I}_{T/X}\,\sigma_{cxx}$; $\sigma_{\ell 12} = \mathcal{I}_{S/X}\,\sigma_{cxx}$

AND AT FAILURE $\sigma_{cxx} = S_{cxx}$

Figure 8. - Ply stress influence coefficients.

$$F(\sigma_\ell, S_\ell, E_\ell, \mathcal{F}_{HTM}) = 1 - \frac{\sigma_{cxx}^2 E_{\ell 11}^2}{E_{cxx}^2} \left\{ \frac{1}{S_{\ell 11a}^2} \left[ (1 - \nu_{\ell 21}\nu_{cxy}) \cos^2\theta + (\nu_{\ell 21} - \nu_{cxy}) \sin^2\theta \right]_\alpha^2 \right.$$

$$+ \frac{\mathcal{F}_m^2 E_{\ell 22}^2}{\mathcal{F}_{HTM}^2 E_{\ell 11}^2 S_{\ell 22\beta}^2} \left[ (\nu_{\ell 12} - \nu_{cxy}) \cos^2\theta + (1 - \nu_{cxy}\nu_{\ell 21}) \sin^2\theta \right]_\beta^2$$

$$+ \frac{\mathcal{F}_m^2 G_{\ell 12}^2}{\mathcal{F}_{HTM}^2 E_{\ell 11}^2 S_{\ell 12s}^2} \left[ (1 + \nu_{cxy}) \sin^2\theta \right]_s^2$$

$$- \frac{K_{\ell 12} \mathcal{F}_m E_{\ell 22}}{E_{\ell 11} S_{\ell 11\alpha} \mathcal{F}_{HTM} S_{\ell 22\beta}} \left[ (1 - \nu_{\ell 12}\nu_{cxy}) \cos^2\theta + (\nu_{\ell 21} - \nu_{cxy}) \sin^2\theta \right]_\alpha$$

$$\left. \times \left[ (\nu_{\ell 12} - \nu_{cxy}) \cos^2\theta + (1 - \nu_{cxy}\nu_{\ell 21}) \sin^2\theta \right]_\beta \right\}$$

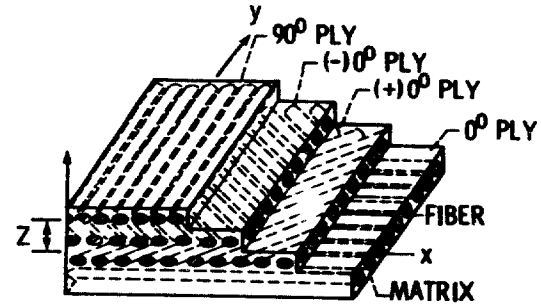


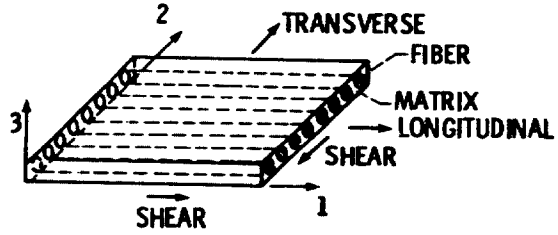


$$\mathcal{F}_m = \left[ \frac{T_{gw} - T}{T_{go} - To} \right]^{1/2} ; \quad \mathcal{F}_{HTM} = \mathcal{F}_m - B \log_{10} N$$

Figure 9. - Ply combined stress failure criterion with hygrothermomechanical effects.

TRANSVERSE STRENGTH

$$S_{\ell 22} = (1 - \sqrt{k_f})\,\phi_{HTM}\,S_m \approx C_s\,S_m$$

IF $S_m = \lambda_s S_{mo} \quad (\lambda_s > 1)$

$$S_{\ell 22} \approx C_s \lambda_s S_{mo}$$

TRANSVERSE MODULUS

$$E_{\ell 22} = \frac{\phi_m E_m}{1 - \sqrt{k_f}\left(1 - \frac{\phi_m E_m}{E_{f22}}\right)} \approx C_m E_m$$

$$E_m = \lambda_m E_{mo} \quad (\lambda_m > 1)$$

$$E_{\ell 22} = C_m \lambda_m E_{mo}$$

ENERGY DENSITY

$$U_{\ell 22} = \frac{S^2_{\ell 22}}{2E_{\ell 22}} = \frac{C_s^2 \lambda_s S^2_{mo}}{2C_m \lambda_m E_{mo}}$$

FIRST PLY FAILURE

$$S_{cxx} = \left\{ \frac{C_o \phi_m (1 - k_f)\left[1 - \sqrt{k_f}\left(1 - \frac{\phi_m E_m}{E_{f22}}\right)\right]}{\phi_m} \right\} \frac{S_m}{E_m}$$

$$S_{cxx} \approx C\,\frac{\lambda_s S_{mo}}{\lambda_m E_{mo}}$$

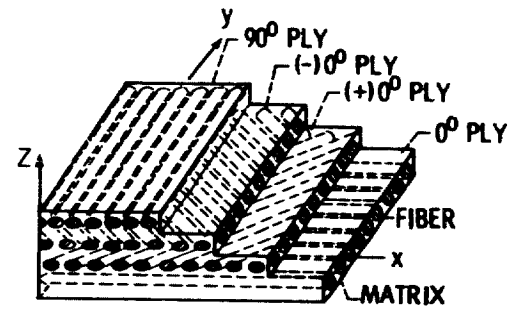


Figure 10. - Benefit bounds equations for resin properties.

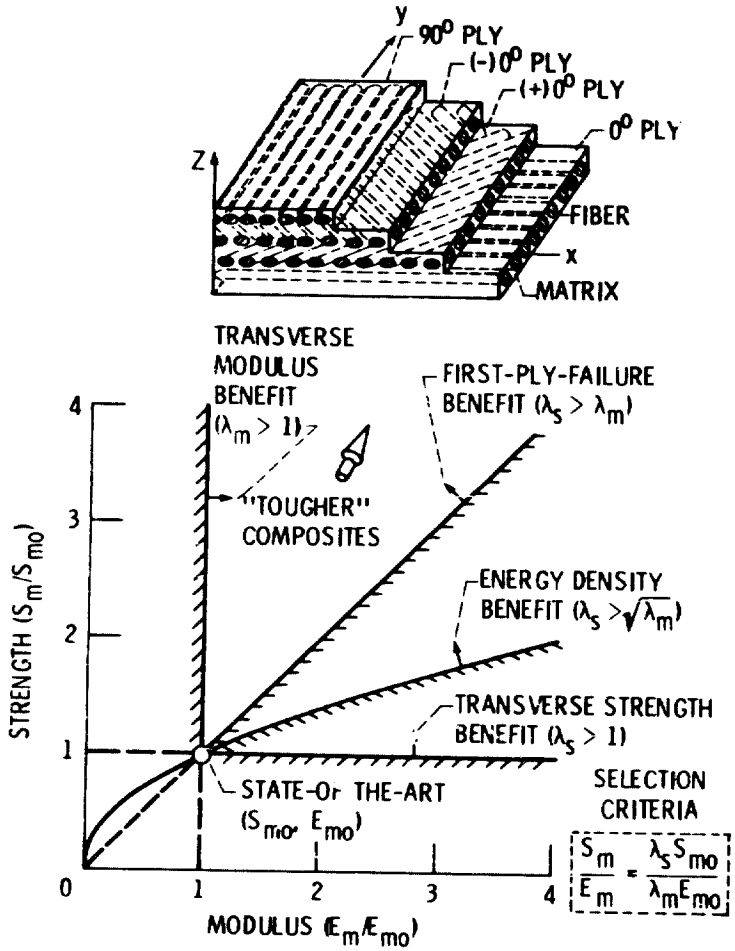


Figure 11. - Resin selection criteria for "tougher" composites.

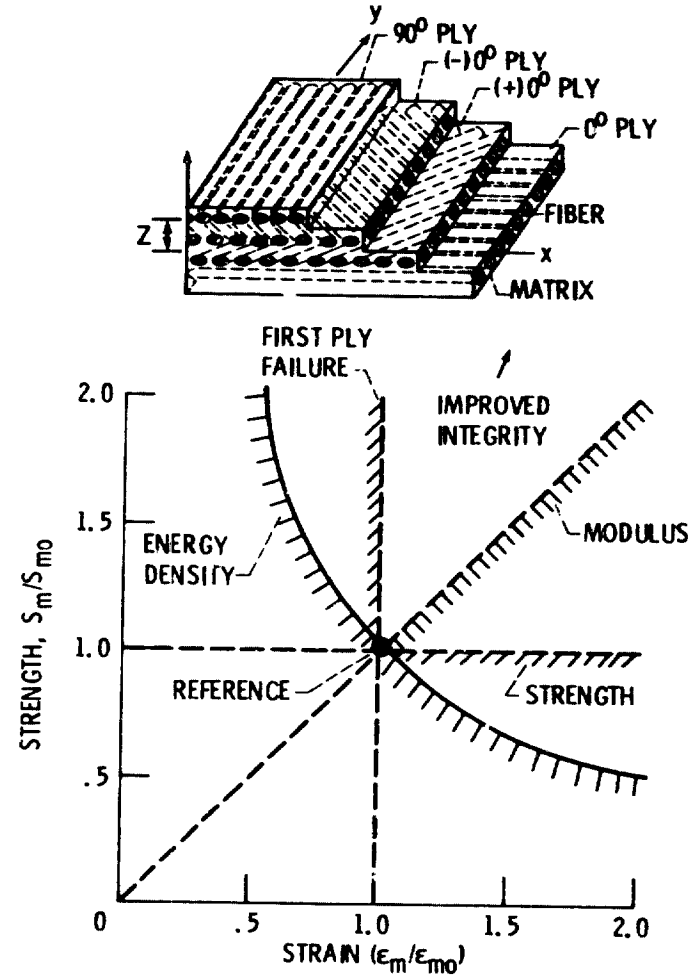


Figure 12. - Resin property regions for improved composite structural integrity.

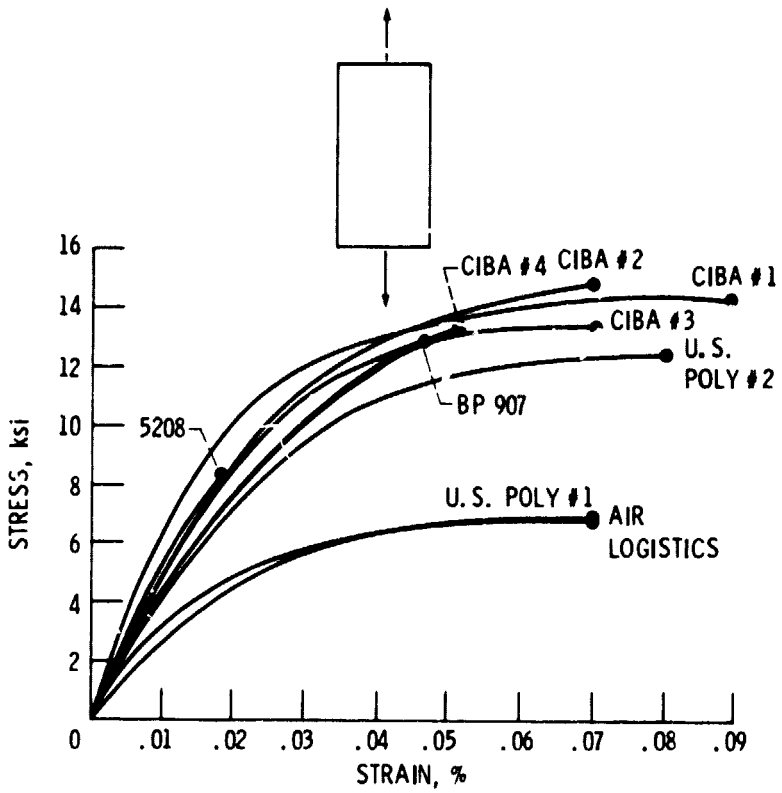


Figure 13. - Average results of tough resin stress-strain curves.

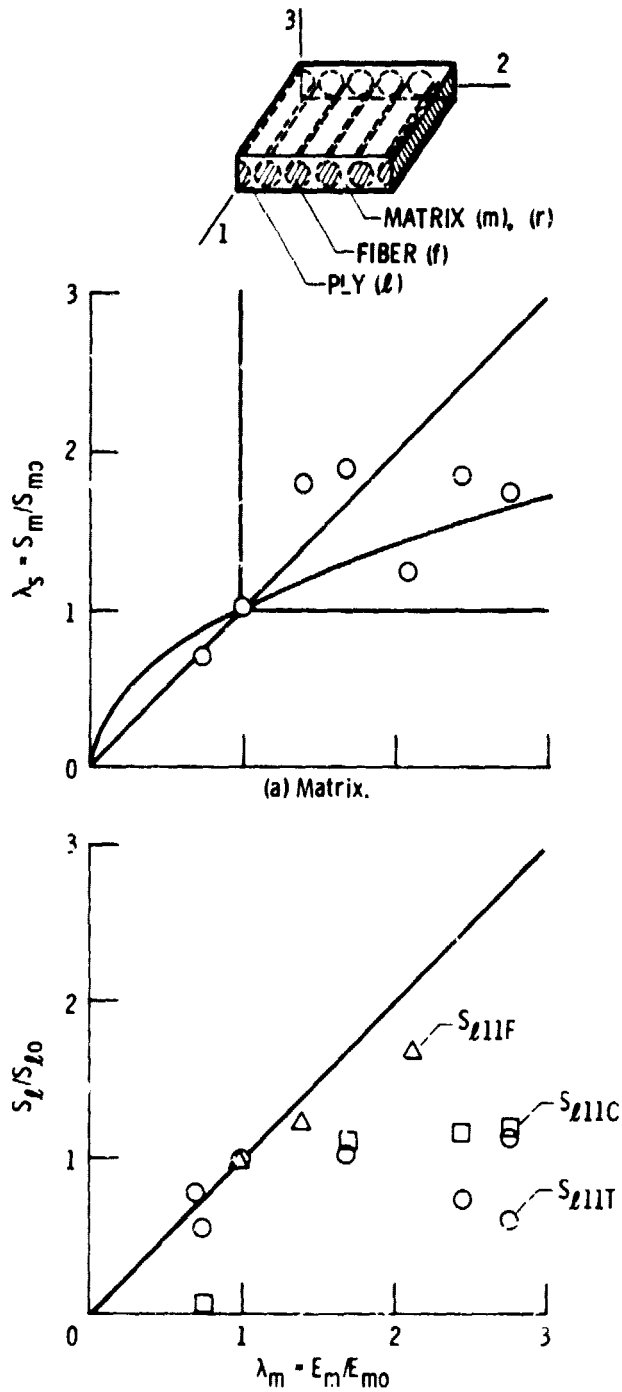


Figure 14. - Resin selection criteria correlation with measured composite data.

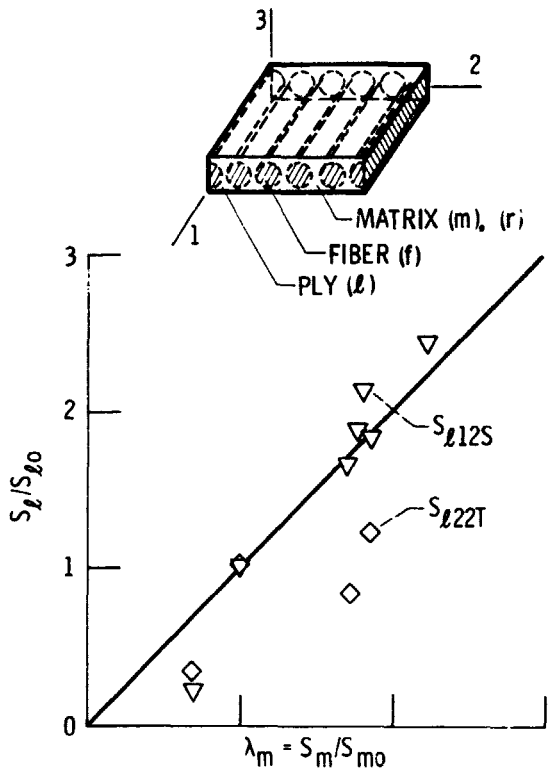


(c) Unidirectional composite transverse and shear.

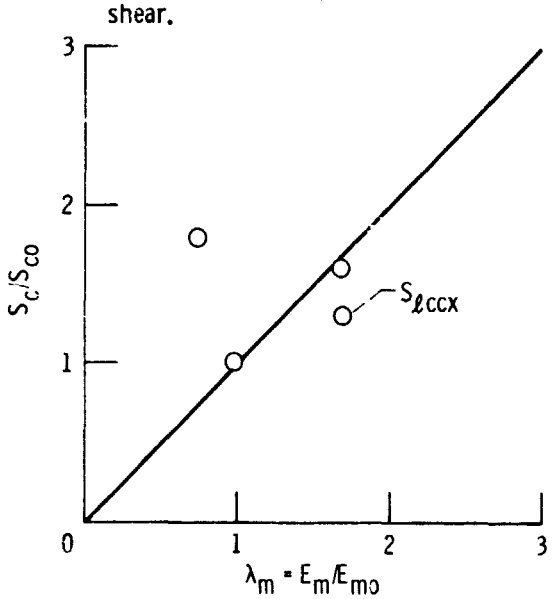


(d) $[0_2/\pm 45]_s$ laminate.

Figure 14. - Concluded.

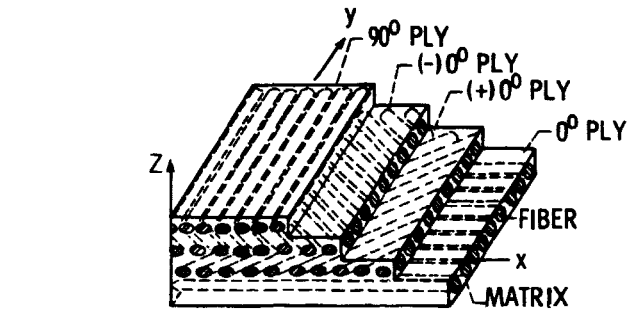


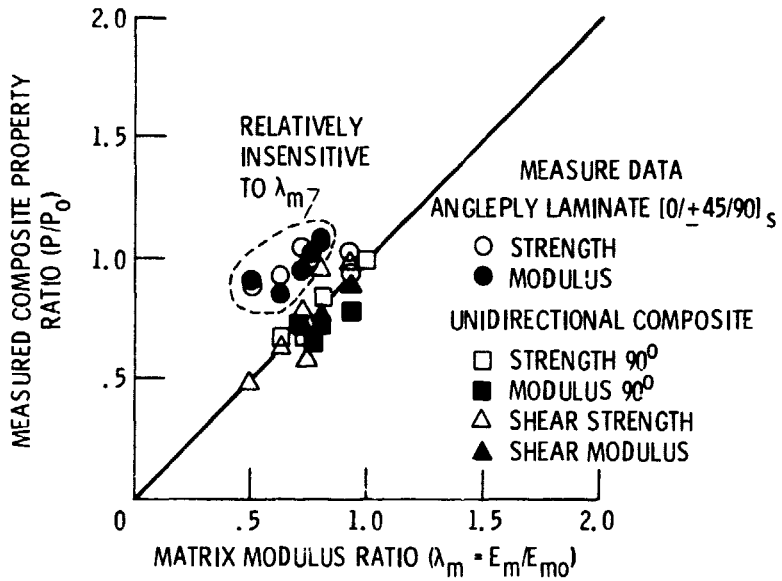


Figure 15. - Proposed resin selection criteria correlate with measured data. $P_o$ and $E_{mo}$ are reference properties.

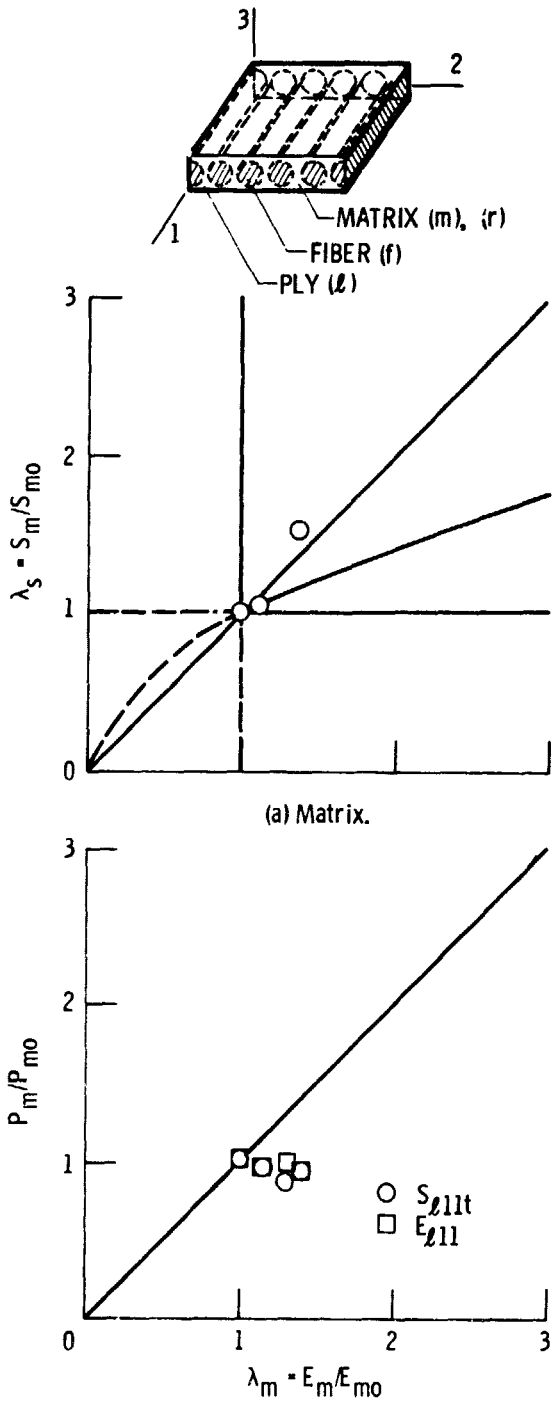


Figure 16. - Resin selection criteria correlation with measured composite data at elevated temperature.

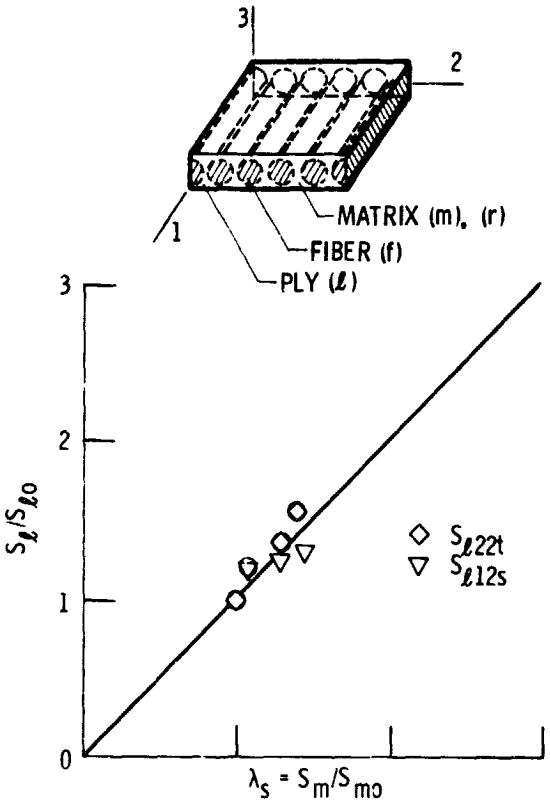


(c) Unidirectional composite transverse and shear.

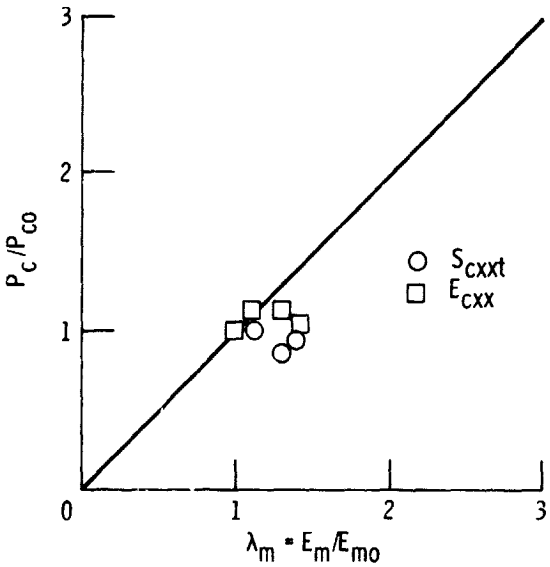


(d) $[0/\pm45/90]_s$ laminate.

Figure 16. - Concluded.

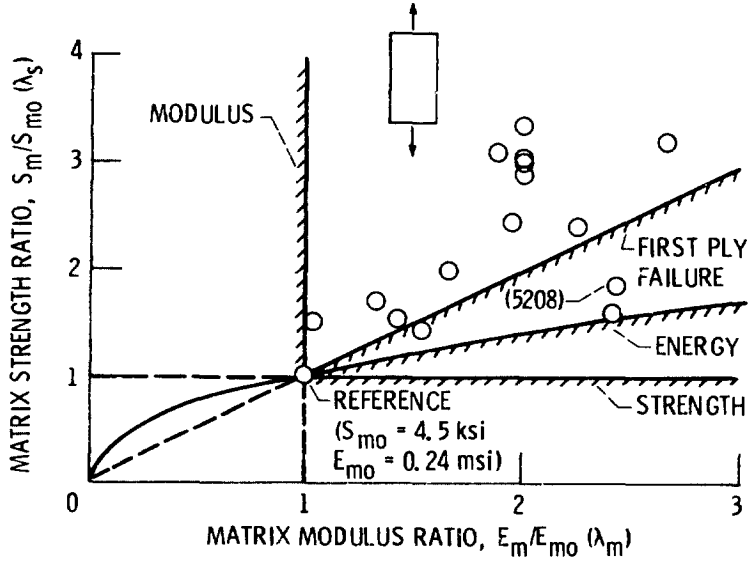


Figure 17. - Measured resin properties on selection criteria space.

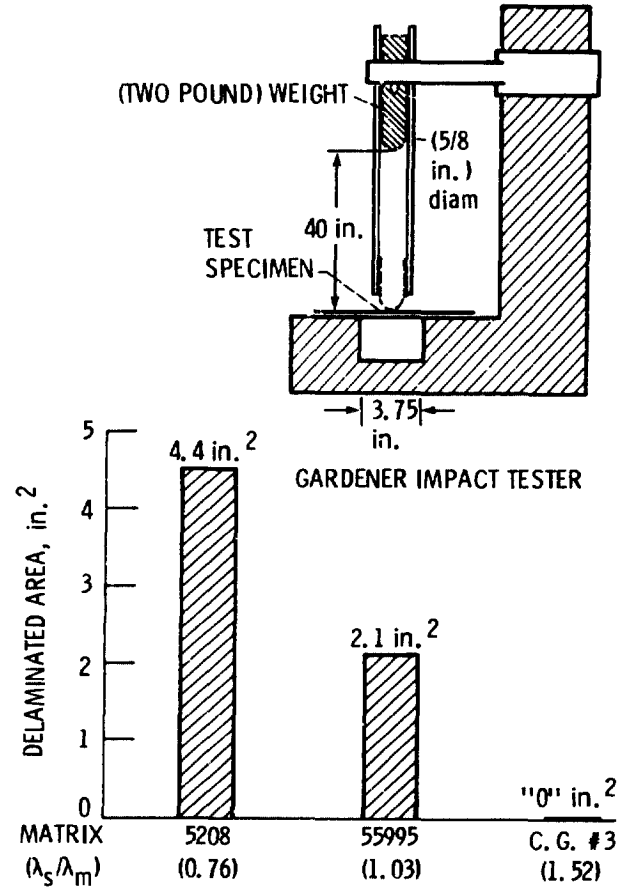


Figure 18. - Resin selection criteria correlation with impact-induced delaminated area, $([0/\pm45/90]_S$ T300/resin).